Multi-Qubit Systems: Highly Entangled States and Entanglement Distribution

A. Borras[1], A.R. Plastino[1,2,3*], J. Batle[1], C. Zander[2], M. Casas[1], and A. Plastino[3]

[1] *Departament de Física and IMEDEA-CSIC,*

Universitat de les Illes Balears, 07122 Palma de Mallorca, Spain

[2] *Physics Department, University of Pretoria, Pretoria 0002, South Africa*

[3] *National University La Plata and Conicet,*

Casilla de Correo 727, La Plata 1900, Argentina.

(Dated: March 27, 2008)

Abstract

A comparison is made of various searching procedures, based upon different entanglement measures or entanglement indicators, for highly entangled multi-qubits states. In particular, our present results are compared with those recently reported by Brown et al. [J. Phys. A: Math. Gen. 2005 **38** 1119]. The statistical distribution of entanglement values for the aforementioned multi-qubit systems is also explored.

keywords: Multi-Qubit Systems, Quantum Entanglement

* Corresponding Author: arplastino@maple.up.ac.za

I. INTRODUCTION

Quantum entanglement [1] is nowadays regarded as constituting one of (if not the) most basic features of quantum mechanics [2, 3, 4]. The increasing interest generated by this subject within the research community [5, 6, 7, 8, 9, 10, 11, 12, 13, 14, 15, 16, 17, 18, 19, 20, 21, 22, 23, 24, 25, 26, 27] has been greatly stimulated by the discovery of novel quantum information processes [2, 3, 4] (such as quantum teleportation and superdense coding) that may lead to important practical developments. The technological relevance of quantum entanglement is not limited to the information technologies, but is also at the basis of other interesting applications, such as quantum metrology [5]. Besides its remarkable technological impact, current research in quantum entanglement is contributing to a deeper understanding of various basic aspects of quantum physics, such as, for instance, the foundations of quantum statistical mechanics [6, 7]. The relationship between entanglement and the dynamical evolution of multipartite quantum systems [8, 9, 10, 11] constitutes another interesting example.

Due to its great relevance, both from the fundamental and from the practical points of view, it is imperative to explore and characterize all aspects of the quantum entanglement of multipartite quantum systems. A considerable amount of research has recently been devoted to the study of multi-qubit entanglement measures defined as the sum of bipartite entanglement measures over all (or an appropriate family of) the possible bi-partitions of the full system [14, 15, 17, 18, 19, 20, 21, 22, 23, 24, 25, 26] (see also [27] for another approach, also based on bi-partitions, to multi-artite entanglement). In particular, Brown et al. [14] have performed a numerical search of multi-qubit states exhibiting a high value of an entanglement measure defined in the aforementioned way, based upon the negativity of the system's bi-partitions. The purpose of the present work is twofold. On the one hand, we numerically determine the distribution of entanglement values (according to four different measures of multi-qubit entanglement based upon bi-partitions) of pure states of three, four, and five qubits, and its relationship with important particular states, such as the $|GHZ\rangle$ state. On the other hand, we report the result of running numerical searches of multi-qubit states (up to 7 qubits) exhibiting high entanglement according to the alluded to four measures. The results obtained using each of these four measures are compared to each other, and also compared to those reported by Brown et al. [14].

The paper is organized as follows. Some basic properties of the entanglement measures used here are reviewed in Section II. Our results concerning the distribution of multi-qubit entanglement measures for systems of 3, 4, and 5 qubits are reported and discussed in Section III. Our algorithm for the search of states of high entanglement is presented in Section IV, and the main results obtained are discussed and compared with those reported by Brown et al. Finally, some conclusions are drawn in Section V.

II. PURE STATE MULTIPARTITE ENTANGLEMENT MEASURES BASED ON THE DEGREE OF MIXEDNESS OF SUBSYSTEMS

Research on the properties and applications of multipartite entanglement measures has attracted considerable attention in recent years [14, 15, 17, 18, 19, 20, 21, 22, 23, 24, 25, 26]. One of the first practical entanglement measures for N-qubit pure states $|\phi\rangle$ to be proposed was the one introduced by Meyer and Wallach [17]. It was later pointed out by Brennen [18] that the measure advanced by Meyer and Wallach is equivalent to the average of all the single-qubit linear entropies,

$$Q(|\phi\rangle) \;=\; 2\left(1-\sum_{k=1}^{N} tr\rho_k^2\right). \tag{1}$$

where $\rho_k,\ \ k=1,\ldots N$, denotes the marginal density matrix describing the kth qubit of the system after tracing out the rest. This quantity, often referred to as "global entanglement" (GE), describes the average entanglement of each qubit of the system with the remaining $(N-1)$-qubits. The GE measure is widely regarded as a legitimate, useful and practical N-qubit entanglement measure [18, 19, 20, 21, 22]. This measure is invariant under local unitary transformations and non-increasing on average under local quantum operations and classical communication. That is to say, Q is an entanglement monotone. Another interesting feature of this measure is that it can be determined without the need for full quantum state tomography [18]. This measure proved to be useful in the study of several problems related to multipartite entanglement, such as entanglement generation by nearly random operators [19] and by operators characterized by special matrix element distributions [20], thermal entanglement in multi-qubit Heisenberg models [21], and multipartite entanglement in one-dimensional time-dependent Ising models [22]. Other entanglement measures, based upon the average values of the linear entropies associated with more general partitions of

the N-qubit systems into two subsystems (that is, involving not only the partitions of the system into a 1-qubit subsystem and an $(N-1)$-subsystem) have also been recently explored [23, 24, 25]. In particular, Scott [23] studied various interesting aspects of the family of multiqubit entanglement measures given by

$$Q_m(|\phi\rangle) = \frac{2^m}{2^m-1}\left(1-\frac{m!(N-m)!}{N!}\sum_s tr\rho_s^2\right), \quad m=1,\ldots,[N/2], \tag{2}$$

where the sum is taken over all the subsystems s constituted by m qubits, ρ_s are the concomitant marginal density matrices, and $[x]$ is the integer part of x. The quantities Q_m correspond to the average entanglement between subsystems consisting of m qubits and the remaining $N-m$ qubits. The measures Q_m have been applied to the study of quantum error correcting codes and to the analysis of the (multipartite) entangling power of quantum evolutions [23].

Another way of characterizing the global amount of entanglement exhibited by an N-qubit state is provided by the sum of the (bi-partite) entanglement measures associated with the $2^{N-1}-1$ possible bi-partitions of the N-qubits system [14]. These entanglement measures are given, essentially, by the degree of mixedness of the marginal density matrices associated with each bi-partition. These degrees of mixedness can be, in turn, evaluated in several ways. For instance, we can use the von Neumann entropy, the linear entropy, or a Renyi entropy of index q. In what follows we are going to consider the following ways of computing the degrees of mixedness of the marginal density matrices ρ_i,

- The linear entropy $S_L = 1 - Tr[\rho_i^2]$.
- The von Neumann entropy $S_{VN} = -Tr[\rho_i \log_2 \rho_i]$.
- The Renyi entropy with $q \to \infty$, $S_{Re}^{q\to\infty} = -\ln \lambda_k^{max}$, where λ_k are the eigenvalues of the marginal density matrix. This particular instance of the Renyi entropy constitutes the case (within the Renyi family) that differs the most from the von Neumann entropy [28, 29].

Besides these measures we are also going to consider the "negativity" as a measure of the amount of entanglement associated with a given bi-partition. The negativity is given by

$$\text{Neg.} = \sum |\alpha_i|, \tag{3}$$

where α_i are the negative eigenvalues of the partial transpose matrix associated with a given bi-partition. The global, multipartite entanglement measures associated with the sum (over all bi-partitions) of each of these four quantities are here going to be denoted, respectively, by E_L, E_{VN}, E_R, and E_N.

Upper bounds for the four entanglement measures E_L, E_{VN}, E_R, and E_N can be established by considering an (hypothetical) N-qubits pure state such that all its marginal density matrices are fully mixed. These bounds can be seen in Table 1. Notice, however, that these bounds may not be reachable. For instance, there is no four qubit state reaching the alluded bound [15].

N	3	4	5	6	7
$E_{L,max}$	1.5	4.25	10	23	49.875
$E_{VN,max}$	3	10	25	66	154
$E_{Re,max}$	2.07944154	6.93147181	17.3286795	45.7477139	106.744666
$E_{Neg,max}$	1.5	6.5	17.5	60.5	157.5

TABLE I: Upper bounds for the entanglement measures E_L, E_{VN}, E_R, and E_N.

III. DISTRIBUTION OF MULTIQUBIT ENTANGLEMENT

In this section we determine numerically the distribution of entanglement values corresponding to pure states of multi-qubit systems randomly generated according to the Haar measure. In Figures 1, 2, and 3 we plot (for systems of 3, 4, and 5 qubits respectively) the probability densities P of finding multi-qubit states with given values of the entanglement measures E_L, E_{VN}, E_R, and E_N. In these Figures we also show vertical lines corresponding to the entanglement values of important particular states, such as the N-qubit GHZ state,

$$|GHZ\rangle = \frac{1}{\sqrt{2}}(|0\ldots0\rangle + |1\ldots1\rangle), \tag{4}$$

the states of high entanglement $BSSB4$ and $BSSB5$ (of four and five qubits, respectively) discovered numerically by Brown et al. [14], and the four qubit state HS, that has been

conjectured to maximize the entanglement of four-qubit states [15] (when measuring entanglement using the sum of the marginal von Neumann entropies associated with all bipartitions). The HS state has recently been shown to constitute a local maximum of the E_{VN} entanglement measure for four-qubits states [16].

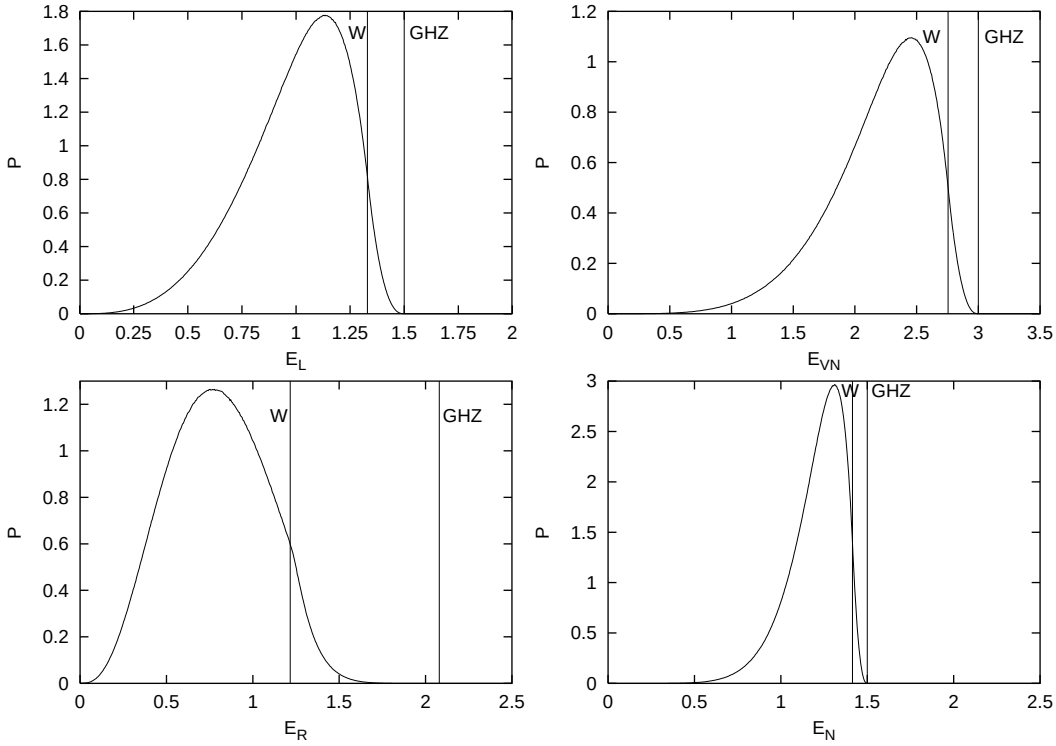

FIG. 1: Entanglement distributions for 3 qubits states. All depicted quantities are dimensionless.

A particularly interesting aspect of Figures 1, 2, and 3 is the status (as far as the present multi-qubit entanglement measures are concerned) of the state GHZ with respect to the bulk of the states of the multi-qubit system.

For three qubits systems, the $|GHZ\rangle$ state has all its single-qubit marginal density matrices complete mixed and, consequently, constitutes the state of maximum entanglement according to the measures E_{VN}, E_L, E_N, and E_R. On the other hand, the state

$$|W\rangle \;=\; \frac{1}{\sqrt{3}}\Big(|100\rangle + |010\rangle + |001\rangle\Big), \tag{5}$$

according to those same measures, exhibits considerably less entanglement than $|GHZ\rangle$. However, as can clearly be appreciated in Figure 1, the W state is still within the most

entangled three-qubit pure states. The W state is clearly more entangled than the "typical" pure state of three qubits.

We have seen that, in the case of three-qubits the four measures E_{VN}, E_L, E_N, and E_R lead to qualitatively similar conclusions in connection with the entanglement of the states GHZ and W as compared with the entanglement exhibited by typical (pure) states. On the contrary, when four-qubit states are considered, each of the aforementioned entanglement measures yields different results. According to E_R, the state $|GHZ\rangle$ still has an amount of entanglement well above most pure states. According to E_L, the state $|GHZ\rangle$ has an entanglement a little above typical. According to E_{VN}, $|GHZ\rangle$ can be said to be (in terms of its entanglement value) still "within the bulk of pure states", but with an amount of entanglement clearly below typical. Finally, according to E_N, the $|GHZ\rangle$ state exhibits less entanglement than most pure states of four qubits. It is also interesting to notice that the state HS exhibits more entanglement than $BSSB4$ when using the measures E_L, E_{VN}, or E_N. On the contrary, $BSSB4$ has a larger value of E_R than HS.

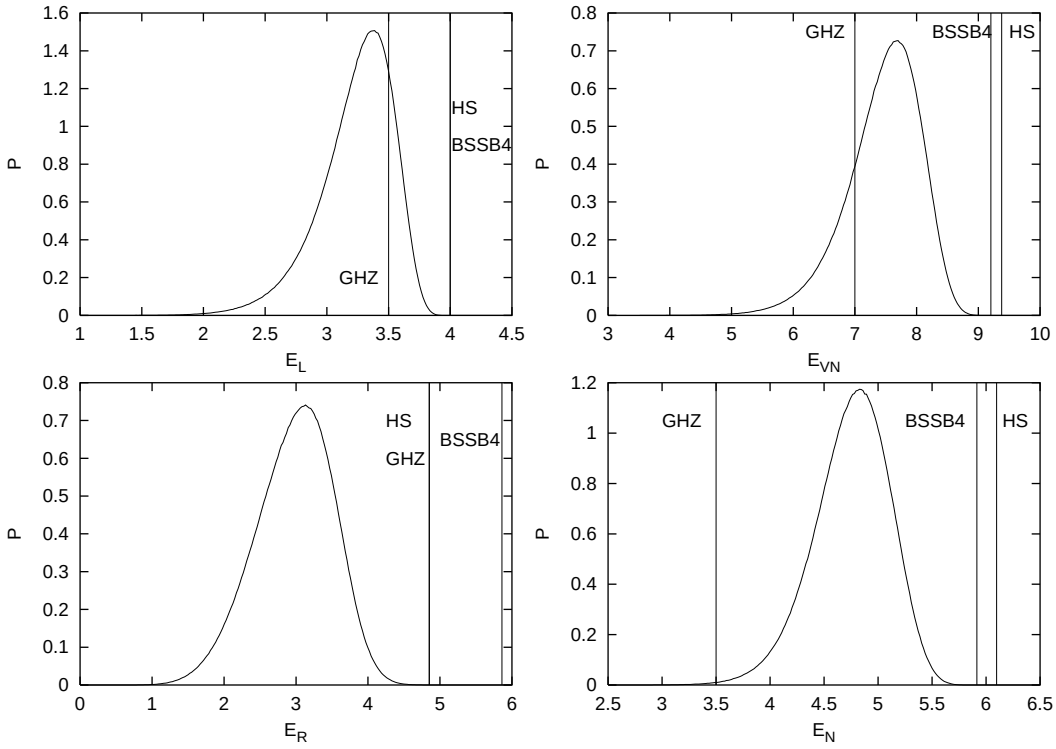

FIG. 2: Entanglement distributions for 4 qubits states. All depicted quantities are dimensionless.

For five-qubit states, the $|GHZ\rangle$ state has less entanglement than most pure states when the entanglement is measured using E_L, E_{VN}, or E_N. Curiously enough, according to E_R

the $|GHZ\rangle$ still ranks as a five-qubit state of rather large entanglement.

IV. SEARCH FOR MULTI-QUBIT STATES OF HIGH ENTANGLEMENT

A. Searching Algorithm

In the present paper we are going to restrict our search of multi-qubit states of high entanglement to *pure states*. In this respect our approach is a little different from that of Brown et al. [14], who considered a search process within the complete space of possible states (that is, with any degree of mixedness). The kind of search studied by Brown et al. is certainly of interest and may shed some light on the structure of the "entanglement landscape" of the full state space. However, it is reasonable to expect the states of maximum entanglement to be pure. Consequently, as far as the search of states of maximum entanglement is concerned, it seems that limiting the search to pure states is not going to reduce its efficiency. The results reported here fully confirm this expectation.

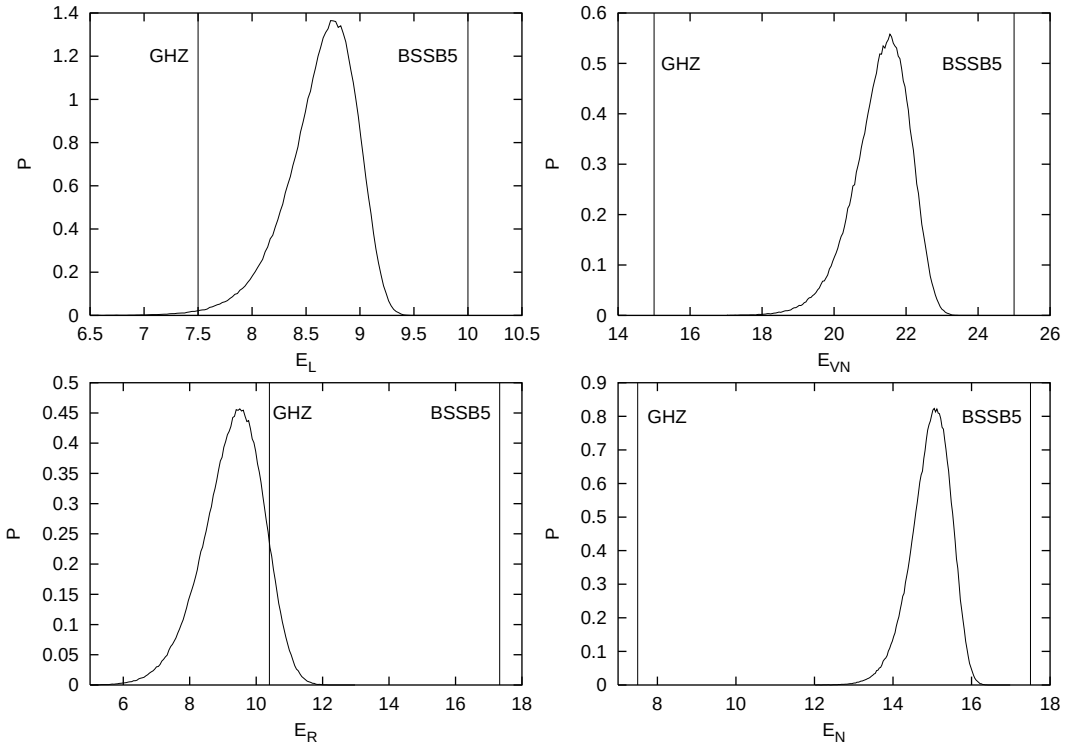

FIG. 3: Entanglement distributions for 5 qubits states. All depicted quantities are dimensionless.

A general pure state of an N-qubit system can be represented as

$$|\Psi\rangle = \sum_{k=1}^{2^N}(a_k + ib_k)|k\rangle, \tag{6}$$

where $|k\rangle$, $(k = 1, \ldots, 2^N)$ represents the states of the computational basis (that is, the 2^N states $|00, \ldots, 0\rangle$, $|10, \ldots, 0\rangle$, $\ldots$, $|11, \ldots, 1\rangle$). We start our search process with the initial state $|000...0\rangle$. In other words, the initial parameters characterizing the state are $a_1 = 1$, and all the rest of the a_i's and b_i's are equal to zero. This initial state is fully factorizable and can thus be regarded as being "very distant" from states of high entanglement. Starting with an arbitrary, random initial pure state does not alter the results of the search process. Now, at each step of the search process a new, tentative state is generated according to the following procedure. A random quantity Δ (uniformly chosen from an interval $(-\Delta_{max}, \Delta_{max})$) is added to each a_i and b_i (a different, independent Δ is generated for each parameter). The new state generated in this way is then normalized to 1 and its entanglement measure is computed. If the entanglement of the new state is larger than the entanglement of the previous state the new state is kept, replacing the previous one. Otherwise, the new state is rejected and a new, tentative state is generated. In order to ensure the convergence of this algorithm to a state of high entanglement, the following two rules are also implemented,

- If 500 consecutive tentative new states are rejected, the interval for the random quantity Δ is changed according to $\Delta_{max} \rightarrow \frac{\Delta_{max}}{2}$ (as the initial value for Δ_{max} we take $\Delta_{max}^{init} = 0.1$).
- When a value $\Delta_{max} \leq 1 \cdot 10^{-8}$ is reached the search program halts.

B. Results Yielded by the Searching Algorithm

The maximum entanglement values obtained from the searching algorithm are listed in Table 2. It must be stressed that the maximum values associated with different measures do not necessarily correspond to the same state. The states obtained when maximizing one particular measure do not exhibit, in general, a maximum value of the other measures. The results obtained by us after running the search algorithm several times (considering the entanglement measures E_L, E_{VN}, E_R, and E_N) can be summarized as follows,

- Among the four measures considered here, E_L is computationally the easiest and quickest to evaluate. The algorithm runs faster when maximizing this measure than

when maximizing any of the other three. However, in the case of four-qubits most states that maximize E_L do not maximize the other measures. There are *many* different four qubit states that exhibit the observed maximum value $E_L = 4$. Few of these states exhibit also the maximum value of the other entanglement measures (for instance, the value $E_{VN} = 9.37734$).

- The measure E_{VN} is computationally more expensive than E_L. The states obtained maximizing E_{VN} also maximize E_L and E_N. In other words, all the states that we have found that realize the observed maximum value of E_{VN} realize as well the observed maxima of E_L and E_N. On the contrary. for four qubits there are many states exhibiting the observed maximum value of E_L that do not reach the observed maxium value of E_{VN}.

- The measure E_R seems to be the "worst" of the four. States that maximize E_R do not, in general, maximize the other measures. And, conversely, states maximizing any of the other measures do not in general maximize E_R.

- E_N is, by far, computationally the most expensive of the measures considered here. The states maximizing this measure also maximize E_L and E_{VN}. In this case the situation is similar to the already mentioned one corresponding to the measure E_{VN}.

	3 qubits	4 qubits	5 qubits	6 qubits	7 qubits
E_L	1.500000	4.00000	10.000000	23.000000	49.573765
E_{VN}	3.000000	9.37734	25.000000	66.000000	152.620140
E_R	2.079441	5.99547	17.328678	45.747705	91.651820
E_N	1.500000	6.09807	17.500000	60.500000	155.812856

TABLE II: Numerically obtained maximum values for the entanglement measures E_L, E_{VN}, E_R, and E_N.

The numerical values reported in the above Table are the result of several search experiments that can be summarized as follows. In the case of three qubits the numerical

optimization of any of the aforementioned measures leads to the same state, the $|GHZ\rangle$ state, and to the concomitant maxima of the entanglement measures. For four qubits, the search for states optimizing E_{VN} yields a final state (equivalent to the $|HS\rangle$ state) that also maximizes all the entanglement measures considered excepting E_R (here, by "equivalent to the $|HS\rangle$ state" we mean that all the marginal density matrices of the alluded state exhibit the same entropic values as those exhibited by the corresponding marginal density matrices of $|HS\rangle$, and also that the alluded state has, for all bipartitions, the same negativities as $|HS\rangle$). The maximum value of E_R reported in Table 2 is generated by search experiments maximizing this entanglement measure. The explicit expression of the corresponding four qubits state is given in the Apendix. The four qubit state obtained when searching for the maximum value of E_N is equivalent to the one obtained when maximizing E_{VN}. When conducting search experiments for four qubit states maximizing E_L we obtain, in most cases, states that do not reach the observed maxima of the rest of the measures. These states are not, in general, equivalent to each other. In point of fact, a different state is obtained in each run of the algorithm optimizing E_L.

The five qubits case is similar to the three qubits one. The numerical search of five qubit states optimizing any of the aforementioned entanglement measures leads to states that exhibit the observed maxima of all these measures (which are reported in Table 2). In other words, if one runs a search algorithm based upon any one of these measures, one obtains a state that exhibits all the maximum entanglement values reported in Table 2. These values are the ones corresponding to the five qubits state (8).

For six qubits, the search experiments based on the maximization of either E_L or E_{VN} lead to final states exhibiting the same values of the four entanglement measures, which are reported in Table 2. The search algorithm based upon the optimization of E_R yields states with lower values of the four measures than those shown in Table 2. For six qubits the search algorithm corresponding to E_N is too slow and we were not able to reach the optimal state.

Finally, in the case of seven qubits the values reported on Table 2 were evaluated on the state found when numerically optimizing E_{VN} (this state is explicitly given in the Appendix). When running numerical searches for seven qubit states optimizing other measures we did not find states with entanglement values higher than those evaluated upon the state obtained when optimizing E_{VN}.

Let us now discuss in more detail the numerically found states of high entanglement.

1. Four Qubits

In the case of four-qubit systems, the extremalization processes based upon either of the measures E_{VN} or E_N always lead to states having the same entanglement values as those exhibited by the HS state discovered by Higuchi and Sudbery [15], which is given by

$$|HS\rangle \;=\; \frac{1}{\sqrt{6}}\Big[|1100\rangle + |0011\rangle + \omega\Big(|1001\rangle + |0110\rangle\Big) + \omega^2\Big(|1010\rangle + |0101\rangle\Big)\Big], \qquad (7)$$

with $\omega = -\frac{1}{2} + \frac{\sqrt{3}}{2}$. We repeated the search process starting with different, random initial conditions and always found states with entanglement values corresponding to the HS state. This constitutes convincing numerical evidence that the HS state is, at least, a local maximum of *both* the E_{VN} and the E_N measures. In fact, it was recently proven by Brierley and Higuchi that the HS state is indeed a local maximum for E_{VN} [16]. Higuchi and Sudbery [15] have provided analytical arguments supporting the conjecture that the HS state is also a *global maximum* for E_{VN}, but this conjecture has not been proven yet. These authors have also proved that there is no pure state of four qubits such that all its two-qubit marginal density matrices are completely mixed [15]. It is interesting that Brown et al. [14], when performing a search process similar (but not identical) to the one considered here, obtained instead of the HS state always a state (which we here call $BSSB4$) exhibiting values of E_{VN} and E_N smaller than those exhibited by HS. Besides some intrinsic differences in the algorithm itself, there is the fact that the main results reported here were computed starting the search process with a pure state, while Brown et al. started their search with a mixed state. It is also worthwhile mentioning that we performed the searches using a FORTRAN program, while Brown et al. employed a MAPLE program. When running a search algorithm maximizing the E_L measure, we obtained several different final states, some of them exhibiting values of E_{VN} larger than the value corresponding to the state $BSSB4$. All these findings suggest that, perhaps, the state $BSSB4$ has no special significance (although it certainly is a highly entangled four-qubits state). Its appearance when running the searching scheme developed by Brown et al. seems to be just an accident due to some special features of that algorithm.

We must mention that we also ran a search algorithm (written in the computer language

MATHEMATICA) similar to that of Brown et al. (and different from the one discussed in most of the present paper), obtaining the same results as Brown et al. did (that is, the algorithm converged to a state with entanglement values corresponding to $BSSB4$). On the other hand, when running an algorithm (written in MATHEMATICA) exhibiting the same basic structure of our FORTRAN program we get the same results as those obtained with the FORTRAN code. The main difference between our algorithm (either in the FORTRAN or the MATHEMATICA versions) and the one used by Brown et al. (when particularized to pure states) is the following. When generating new random trial states (in the "pure state version" of Brown et al. algorithm) one choses a random coefficient of the previous state, multiply the corresponding real and imaginary parts by positive random numbers, and re-normalize the state. On the other hand, in our algorithm (see sub-section IV A) *we add random numbers (that may be positive or negative) to the real and imaginary parts of the state's coefficients* (and then re-normalize the state). The results of various numerical experiments done by us suggest that this difference on the implementation of the searching algorithm accounts for the different results obtained for highly entangled four qubits states.

2. Five Qubits

When running our search scheme for states of five qubits, we always obtain states exhibiting the same entanglement values as the state obtained by Brown et al. [14],

$$|BSSB5\rangle \;=\; \frac{1}{2}\Big[|100\rangle|\Phi_-\rangle + |010\rangle|\Psi_-\rangle + |100\rangle|\Phi_+\rangle + |111\rangle|\Psi_+\rangle\Big] \tag{8}$$

where $\Psi_\pm = |00\rangle \pm |11\rangle$ and $\Phi_\pm = |01\rangle \pm |10\rangle$. This state has all its marginal density matrices (for 1 and 2 qubits) completely mixed.

3. Six Qubits

In the case of six qubits, our algorithm converges to highly entangled states exhibiting all the marginal density matrices for states of 1, 2, 3 qubits completely mixed. In particular, we discovered the new state of high entanglement,

$$\Psi_{6qb} = \frac{1}{\sqrt{32}} \Big[|000000> + |111111> + |000011> + |111100> + |000101> + |111010> + |000110> + |111001> + |001001> + |110110> + |001111> + |110000> + |010001> + |101110> + |010010> + |101101> + |011000> + |100111> + |011101> + |100010> - \big(|001010> + |110101> + |001100> + |110011> + |010100> + |101011> + |010111> + |101000> + |011011> + |100100> + |011110> + |100001> \big) \Big] \quad (9)$$

which, to the best of our knowledge, has not yet been reported in the literature. This state has a rather simple structure, with all its coefficients (when expanded in the computational basis) equal to 0 or ± 1 (the same situation occurs for maximally entangled states of 2, 3, 4, and 5 qubits).

4. 7 qubits

When we ran the search program for seven-qubit states of high entanglement we found states with the following features. They all have completely mixed single qubit marginal density matrices. However, these states do not exhibit completely mixed two-qubit and three-qubit marginal density matrices (in this sense, the present situation seems to have some similarities with the four-qubit case).

The high entanglement states of seven qubits that we found are characterized by two-qubits marginal density matrices exhibiting the following entropic values

$$1 - Tr(\rho_i^2) = 0.7445111988 \quad (10)$$

$$S_{VN}(\rho_i) = 1.9841042 \quad (11)$$

$$S_{Re}^{q \to \infty}(\rho_i) = 1.248122309. \quad (12)$$

The three-qubit marginal density matrices of these seven-qubit states have,

$$1 - Tr(\rho_i^2) = 0.86209018886 \quad (13)$$

$$S_{VN}(\rho_i) = 2.93739788 \quad (14)$$

$$S_{Re}^{q\to\infty}(\rho_i) = 1.4712659418. \tag{15}$$

When running our program (maximizing either E_{VN} or E_N) for five-qubit or six-qubit states, *the search process always leads to a state whose marginal density matrices of 1,2, and (in the six-qubit case) 3 qubits are completely mixed*. On the contrary, this never happens when running our algorithm for seven-qubits states. The marginal density matrices of 1 qubit subsystems turn out to be maximally mixed, but not the marginal density matrices corresponding to subsystems consisting of 2 or 3 qubits. Moreover, all the runs of the algorithm for seven-qubits states yielded states with the same entropic values for the marginal statistical operators. This suggests that the case of seven qubits may have some similarities with the case of four qubits. In other words, our results constitute numerical evidence supporting the

Conjecture 1: *There is no pure state of seven qubits whose marginal density matrices for subsystems of 1, 2, or 3 qubits are all completely mixed.*

5. The Single-Qubit Reduced States Conjecture

It was conjectured by Brown et al. [14] that multi-qubit states of maximum entanglement always have all their single-qubit marginal density matrices completely mixed. The results obtained by us when running the search algorithm maximizing the E_{VN} and E_N measures are consistent with the aforementioned conjecture. All the states yielded by the searching algorithm (up to systems of seven qubits) have maximally mixed single qubit marginal density matrices. Moreover, in the case of 5 qubits all the states obtained also exhibited maximally mixed two-qubits marginal density matrices. In the case of 6 qubits, all the states obtained had completely mixed marginal density matrices of one, two, and three qubits.

V. CONCLUSIONS

In the present effort we have investigated some aspects of the entanglement properties of multi-qubit systems. We have considered global, multi-qubit entanglement measures based upon the idea of considering all the possible bi-partitions of the system. For each bi-partition we computed a bi-partite entanglement measure (such as the von Neumann entropy of the marginal density matrix associated with the subsystem with a Hilbert space

of lower dimensionality) and then summed the measures associated with all the bi-partitions. This approach has been widely used in the recent literature. In order to evaluate the bi-partite contributions we considered four different quantities: the von Neumann, linear, and Renyi (with $q \to \infty$) entropies, and the negativity. Consequently, we have considered four entanglement measures.

We determined numerically, for the aforementioned four measures, the distributions of entanglement values in the Hilbert spaces of pure states of three, four, and five qubits. This allowed us to determine, for instance, the entanglement status of special states (such us the $|GHZ\rangle$ state) with respect to the bulk of the state space.

We also determined, for systems of four, five, six and seven qubits, states of high entanglement using a search scheme akin, but not identical to, the one recently advanced by Brown et al. [14]. These authors performed the search process using an entanglement measure based on the negativity. We investigated the behavior of the search processes based on four different measures: the negativity, and the von Neumann, linear, and Renyi (with $q \to \infty$) entropies of the marginal density matrices associated with a bi-partition. The results obtained by us have some interesting features when compared with those reported by Brown et all [14]. First of all, we found that a search algorithm based on the von Neumann entropy is as successful as one based upon negativity. However, the von Neumann entropy is (in general) considerably less expensive to compute than the negativity. Consequently, when initializing the search process with a pure state, it is better to use the von Neumann entropy.

In the case of states of four qubits Brown et al. reported that their search algorithm always converged (up to local unitary transformations) to a state (here called the $BSSB4$ state) exhibiting less entanglement than the HS state. On the contrary, our algorithm always converged to states exhibiting the same entanglement measures as those characterizing the HS state. Our results thus provide further support to the conjecture advanced by Higuchi and Sudbery [15] that the HS state corresponds to a global entanglement maximum for four-qubits states. Another interesting finding, going beyond the results of Brown et al. is a particular state of six qubits (discovered using our search algorithm) that has all its marginal density matrices of 1, 2, and 3 qubits completely mixed. It is interesting that (in the computational basis) all the coefficients characterizing this state are (up to a global normalization constant) equal to 0 or ± 1.

Finally, on the basis of the numerical evidence obtained by us when running our search algorithm for highly entangled states of seven qubits, we make the conjecture that there is no pure state of seven qubits whose marginal density matrices for subsystems of 1, 2, or 3 qubits are all completely mixed.

Acknowledgements

This work was partially supported by the MEC grant FIS2005-02796 (Spain) and FEDER (EU) and by CONICET (Argentine Agency). The financial assistance of the National Research Foundation (NRF; South African Agency) towards this research is hereby acknowledged. Opinions expressed and conclusions arrived at, are those of the authors and are not necessarily to be attributed to the NRF. A. Borrás acknowledges support from the FPU grant AP-2004-2962 (MEC-Spain).

---

[1] Bengtsson I and Zyczkowski K 2006 *Geometry of Quantum States: An Introduction to Quantum Entanglement* (Cambridge: Cambridge University Press)

[2] Nielsen N and Chuang I L 2000 *Quantum Computation and Quantum Information* (Cambridge: Cambridge University Press)

[3] Lo H-K, Popescu S and Spiller T (Eds) 1998 *Introduction to Quantum Computation and Information* (River Edge: World Scientific)

[4] Bouwmeester D, Ekert A and Zeilinger A (Eds) 1998 *The Physics of Quantum Information* (Berlin: Springer-Verlag)

[5] Giovannetti V, Lloyd S and Maccone L 2006 *Phys. Rev. Lett.* **96** 010401

[6] Gemmer J, Michel M and Mahler G 2004 *Quantum Thermodynamics* (Berlin: Springer-Verlag)

[7] Popescu S, Short A J, and Winter A 2006 *Nature Physics* **2** 754

[8] Giovannetti V, Lloyd S and Maccone L, 2003 *Europhys. Lett.* **62** 615-621

[9] Giovannetti V, Lloyd S and Maccone L 2003 *Phys. Rev. A* **67** 052109

[10] Batle J, Casas M, Plastino A and Plastino A R 2005 *Phys. Rev. A* **72** 032337

[11] Borras A, Casas M, Plastino A R and Plastino A 2006 *Phys. Rev. A* **74** 022326

[12] Bennett C H, Popescu S, Rohrlich D, Smolin J A and Thapliyal A V 2000 *Phys. Rev. A* **63** 012307

[13] Batle J, Casas M, Plastino A and Plastino A R 2005 *Phys. Rev. A* **71** 024301

[14] Brown I D K, Stepney S, Sudbery A and Braunstein S L 2005 *J. Phys. A: Math. Gen.* **38** 1119

[15] Higuchi A and Sudbery A 2000 *Phys. Lett. A* **273** 213-217 (Preprint quant-ph 0005013)

[16] Brierley S and Higuchi A 2007 *J. Phys. A: Math. Gen.* **40** 8455

[17] Meyer D A and Wallach N R 2002 $\widehat{\text{J}}$. Math. Phys. **43** 4273

[18] Brennen G K 2003 *Quantum Inf. Comput.* **3** 619

[19] Weinstein Y S and Hellberg C S 2005 *Phys. Rev. Lett.* **95** 030501

[20] Weinstein Y S and Hellberg C S 2005 *Phys. Rev. A* **72** 022331

[21] Cao M Zhu S 2005 *Phys. Rev. A* **71** 034311

[22] Lakshminarayan A and Subrahmanyam V 2005 *Phys. Rev. A* **71** 062334

[23] Scott A J 2004 *Phys. Rev. A* **69** 052330

[24] Carvalho A R R, Mintert F and Buchleitner A 2004 *Phys. Rev. Lett.* **93** 230501

[25] Aolita M and Mintert F 2006 *Phys. Rev. Lett.* **97** 050501

[26] Calsamiglia J, Hartmann L, Durr W and Briegel H-J 2005 *Phys. Rev. Lett.* **95** 180502

[27] Facchi P, Florio G and Pascazio S 2006 *Phys. Rev. A* **74** 042331

[28] Batle J, Casas M, Plastino A R and Plastino A 2002 *Phys. Lett. A* **296** 251

[29] Batle J, Casas M, Plastino A R and Plastino A 2003 *Eur. Phys. Journal B* **35** 391

VI. APPENDIX

In this appendix we present the explicit expressions for some of the states that we have introduced in the previous sections. To give the expression of a state $|\Psi\rangle$ we list the values of the coefficients C_i appearing in the expansion $|\Psi\rangle = \sum C_i|i\rangle$ of the alluded state in the computational basis $\{|i\rangle\}$.

TABLE III: Coefficients for the 4 qubit state maximizing the entanglement measure based on the Renyi entropy. This state doesn't maximize any other entanglement measure.

i	C_i
0	(0.337140676904686,0.174693405076796)
1	(3.860442882346969E-002,6.837682483380016E-002)
2	(5.962390590615981E-002,0.130590439038055)
3	(3.780903708091862E-002,0.283134470502957)
4	(0.128308013031141,0.160044519815334)
5	(-4.976588113149925E-002,-0.156794899004251)
6	(0.150158286657780,-0.269632673631216)
7	(-0.284880375838561,4.364132887880368E-002)
8	(-0.291078649973983,-0.122251701129522)
9	(8.597952221078008E-002,-0.132269103402589)
10	(-0.184679774192993,-3.521179357675151E-002)
11	(-7.859668707973404E-002,0.285246180204626)
12	(-3.120148147808102E-002,3.966923168894761E-002)
13	(-0.352475250278756,-0.170787520712258)
14	(2.666941273479068E-002,-0.244143026082971)
15	(0.176830325000684,-7.078443862056820E-002)

TABLE IV: Coefficients for the 7 qubit state maximizing the von Neumann entropy based entanglement measure. It also maximizes the rest of the entanglement measures used along this paper.

i	C_i
0	(1.992268895612789E-002,-2.048153299374923E-002)
1	(5.733894334752334E-002,4.973994982020743E-003)
2	(-4.620635677624599E-002,9.889188153518157E-002)
3	(0.114773068934711,7.803541807299509E-002)
4	(9.358057357464943E-003,8.773453313011471E-002)
5	(-4.517771306482277E-002,7.317172187520525E-002)
6	(7.148596275123295E-002,-6.486415242189469E-002)
7	(8.095549161110917E-002,6.281081599967211E-002)
8	(-0.110934833126726,-6.540485101339541E-002)
9	(4.243711009834195E-002,0.111608997849607)
10	(-5.324057236738998E-002,-1.064133868681598E-002)
11	(-3.199776618312627E-002,1.480812105331856E-002)
12	(-3.484102446829535E-002,6.505443761669717E-002)
13	(6.659331311799828E-002,2.520078454850319E-002)
14	(2.127875261481843E-002,-8.620489194999095E-003)
15	(3.763178050938378E-002,-3.257033322657695E-002)
16	(-9.639113945809372E-002,-8.706895542690339E-002)
17	(7.213494811044056E-002,1.637328607897790E-002)
18	(3.347204156200859E-003,-4.540542385699349E-002)
19	(5.235538552827945E-002,-5.539353156272388E-002)
20	(-5.734329608600269E-002,-3.334326701130044E-002)
21	(-2.042578560682204E-002,-0.106743556238253)
22	(-5.987692237756689E-002,-5.035304599306584E-002)

Continued on next page

TABLE IV – continued from previous page

i	C_i
23	(3.304680530465200E-002,9.449073856519782E-002)
24	(2.843182057391498E-002,-2.453794986457519E-002)
25	(-1.316539219004622E-002,-4.912228258199161E-002)
26	(-5.889102546322750E-002,7.627608399874446E-002)
27	(-9.712149518138669E-002,1.793695100255052E-002)
28	(0.101272862135273,3.940173722756957E-002)
29	(8.351246119258422E-002,-8.055956525511754E-002)
30	(3.447514504354676E-002,-6.113180059952469E-002)
31	(9.951265147314473E-002,5.575638197924940E-002)
32	(-8.560101157107276E-002,4.371001847647850E-002)
33	(1.790860687993339E-002,-4.609380726768647E-002)
34	(0.101094129379701,6.494214772295025E-002)
35	(-2.247063699015752E-002,4.864367215816477E-003)
36	(-0.101021865482900,-3.782742816016475E-002)
37	(3.152510928837363E-002,0.122475737293311)
38	(3.278246037718845E-002,-1.256558150969285E-004)
39	(-5.736492004809834E-002,6.977684817377462E-002)
40	(2.216141448231444E-002,-7.601939988222593E-002)
41	(0.131970698296467,-1.260154440769711E-002)
42	(8.044458687238869E-003,-9.387152676075274E-002)
43	(-7.808462265554876E-003,-1.202931445781517E-002)
44	(-3.274238472614039E-002,-2.514421762607319E-002)
45	(-7.505399199689463E-003,-3.929813385495669E-002)
46	(0.155137227199514,1.049705149755480E-002)
47	(3.965712582027887E-002,1.083231718050668E-002)
48	(-8.224544805028827E-002,-3.383505686446630E-002)
49	(-0.154734489832632,8.673238144109774E-002)

Continued on next page

TABLE IV – continued from previous page

i	C_i
50	(-7.332128812157200E-002,-1.371022464291685E-002)
51	(5.208789441301026E-003,-1.411983814527247E-002)
52	(-3.590001918998145E-002,4.647625796299270E-002)
53	(-8.697459750434891E-004,1.482515294565435E-002)
54	(1.092140821864845E-002,4.129654472949966E-002)
55	(7.674494499478537E-002,-5.338559685445066E-002)
56	(-6.251229029986881E-002,6.425293853541948E-002)
57	(8.520457184967269E-003,-7.709553490818186E-003)
58	(-3.438221523644015E-002,-9.255954127990704E-002)
59	(-2.577383579159245E-002,0.129459058820970)
60	(0.108622543447635,-8.806418991079722E-002)
61	(-8.106072511646092E-003,3.606461883196400E-002)
62	(-1.202677529398651E-002,3.058305163904075E-002)
63	(-2.485595158034444E-002,9.667248785955586E-002)
64	(6.171068243552971E-002,-9.583626876325756E-003)
65	(8.806183494115266E-002,-3.526345160182855E-002)
66	(6.854736532168551E-002,-6.411781011736128E-002)
67	(2.066804256769957E-002,1.612535204191288E-002)
68	(1.438805006820953E-002,0.124162489557811)
69	(-5.074891074532802E-002,-5.439956049423335E-002)
70	(-3.640086957084941E-002,4.594300372342439E-003)
71	(3.550293356508465E-002,8.695740710560376E-002)
72	(-4.773739666022134E-002,-3.667942618866395E-002)
73	(2.346579563123868E-003,-0.119908858816339)
74	(1.493075601025749E-002,4.553124163243615E-002)
75	(5.034836527591473E-002,8.124581001062543E-002)
76	(6.802270653015219E-002,8.317313465161994E-003)

Continued on next page

TABLE IV – continued from previous page

i	C_i
77	(6.283616184316396E-002,6.514992784328244E-004)
78	(0.127829889515795,0.118971821010114)
79	(-9.788293784579458E-002,5.354297473450592E-003)
80	(0.117110474490768,-4.317232032001831E-002)
81	(-9.256055710305476E-002,-2.768362340687266E-002)
82	(-7.244569839572039E-002,6.671389393930190E-002)
83	(-5.515716658607148E-002,2.093262220899585E-002)
84	(-3.028765985082235E-002,4.529684133342195E-002)
85	(-1.454140943294647E-002,7.974409510449305E-002)
86	(-7.121856602606923E-002,-4.438866940874264E-002)
87	(-3.590040749082390E-002,8.143026671780049E-002)
88	(8.912049927583944E-003,-1.389907243324935E-002)
89	(9.484845129641119E-002,-5.878664094021236E-002)
90	(-5.450397076610332E-002,0.117961375334513)
91	(-1.169436871304801E-002,-6.947913611647639E-002)
92	(-6.798510500616832E-002,-7.747559839783932E-002)
93	(1.740724913960769E-002,-1.809038449399666E-002)
94	(-1.885142661877520E-002,6.314493850061739E-002)
95	(7.520470652239290E-002,4.456457191590223E-002)
96	(0.117132792695098,3.066328283226673E-002)
97	(1.127320363030642E-002,-2.083667932069934E-002)
98	(1.977443152287268E-002,4.839368466995119E-002)
99	(-0.146648569587175,-1.841910055111614E-002)
100	(2.485199104080963E-002,-9.065577146599127E-002)
101	(-1.352964224869225E-002,-8.518961930320970E-002)
102	(4.288496230633006E-002,7.033803797783106E-003)
103	(4.876461334642698E-002,-1.428437645902438E-002)

Continued on next page

TABLE IV – continued from previous page

i	C_i
104	(-3.244529712612734E-002,8.121540837139055E-002)
105	(2.809280188171577E-002,4.286033253289921E-002)
106	(5.009488734831499E-002,-6.852953802160539E-002)
107	(-4.883631054660045E-002,6.372960434850038E-002)
108	(-1.583821551197247E-002,-4.855360397290493E-002)
109	(3.537174285397322E-002,0.104311697071161)
110	(4.234833191138120E-002,1.152575018630899E-002)
111	(0.149915848699035,2.063573734200513E-003)
112	(-2.681850738901102E-003,-2.650438998719609E-002)
113	(2.099859642637032E-002,7.483425704168839E-002)
114	(-2.307627608049840E-002,8.294414552141494E-003)
115	(-7.879700573926614E-002,-5.952656546473500E-002)
116	(3.702914401846596E-002,5.284665497817300E-003)
117	(-4.628839981989381E-002,7.345123474109293E-002)
118	(0.107904736635145,-0.164393350587244)
119	(4.763528675022823E-002,1.908136182097281E-002)
120	(0.116908223755807,-4.314878373454251E-002)
121	(3.495914043033557E-002,-4.526014514286658E-002)
122	(6.120391755562234E-002,-3.887547264821206E-002)
123	(3.457915304142278E-002,-7.568701576399368E-002)
124	(6.046688922765979E-002,-3.864792846188141E-002)
125	(-3.215267435226381E-002,0.128788000228012)
126	(-1.191016945303225E-002,3.655884472429104E-003)
127	(-2.612694626117723E-005,-5.303000737423087E-002)